Journal of Applied Polymer Science

Surface modification and immobilization in poly(acrylic acid) of Ag/ZnO for photocatalytic degradation of endocrine-disrupting compounds

Alma Berenice Jasso-Salcedo,[1,2] Dimitrios Meimaroglou,[2] Sandrine Hoppe,[2] Fernand Pla,[2] Vladimir A. Escobar-Barrios[1]

[1]IPICYT, División de Ciencias Ambientales, Camino a la Presa San José 2055, Lomas 4a sección, C.P. 78216, SLP, México

[2]Laboratoire Réactions et Génie des Procédés, UMR 7274, CNRS-Université de Lorraine, Nancy, France

Correspondence to: F. Pla (E-mail: fernand.pla@univ-lorraine.fr)

ABSTRACT: Silver-modified ZnO particles (Ag/ZnO) are effective catalysts for the photodegradation of water pollutants such as bisphenol-A. However, until now, their use in continuous processes was back-drawn because of difficulties associated with their recovery. To overcome this problem, the present work aimed at immobilizing Ag/ZnO in cross-linked poly(acrylic acid) -PAA-. Ag/ZnO was first silanized using (3-glycidyloxypropyl)trimethoxysilane and thoroughly dispersed in a water-acrylic acid solution. The suspension was then submitted to radical polymerization in presence of a cross-linker (N,N′-Methylenebisacrylamide). The resulting composites were characterized in terms of chemical structure, morphology, crystallinity, thermal properties, and photostability. Their analyses showed that the silanized particles were chemically anchored to PAA and homogeneously distributed in the matrix. UV-assisted photocatalysis of bisphenol-A aqueous solutions showed that immobilized Ag/ZnO can achieve photodegradation performances comparable to pure Ag/ZnO and allows its use in successive cycles and, consequently, in continuous processes. © 2016 Wiley Periodicals, Inc. J. Appl. Polym. Sci. **2016**, *133*, 43528.

KEYWORDS: catalysts; composites; degradation; photochemistry; properties and characterization

Received 5 November 2015; accepted 9 February 2016
DOI: 10.1002/app.43528

INTRODUCTION

Among the wide range of natural and man-made substances responsible for the environmental and water pollution, the class of endocrine-disrupting compounds (EDCs) interferes with the body's endocrine system and produces adverse developmental, reproductive, neurological, and immune effects in both humans and wildlife.[1] EDCs may be found in many everyday products, including plastic bottles, metal food cans, detergents, flame-retardants, foods, toys, cosmetics, and pesticides.

Several studies investigated the removal of EDCs and pharmaceuticals from drinking water by biological and adsorption treatments.[1–5] Sunlight-induced degradation of pollutants like EDCs is a very attractive approach for controlling and correcting water pollution.[6] Among the variety of photocatalysts developed for this purpose, TiO_2 is the most frequently used because of its chemical stability, low toxicity, and low cost.[7] However, TiO_2 is photoactive in the UV region because of its higher band gap (3.2 eV), rendering the utilization of solar irradiation meagrely efficient. Because of this, new generations of visible light photocatalysts are under development. Prominent examples include nitrogen-doped TiO_2,[8] plasmonic nanoparticle-TiO_2 composite,[9,10] plasmonic nanoparticle-CuSe,[11] plasmonic nanoparticle-semiconductor,[12–14] and tricomponent photocatalysts.[15,16] In addition, attempts have also been made to design ZnO photocatalysts with effective charge separation and storage of the photoexcited charges. Recently, it has been shown that loading of silver nanoparticles (AgNPs) on ZnO surface can reduce photocorrosion,[17] improve absorption of visible light,[18,19] and increase the photocatalytic efficiency[17–20] of ZnO.

Theoretically, when ZnO is illuminated (e.g., at $\lambda = 384$ nm), the electrons of the valence band are excited to the conduction band, leaving holes behind in the valence band. The electrons are then scavenged by both AgNPs and adsorbed oxygen. Oxygen is usually supplied to form superoxide ions and later hydroxyl radicals (•OH) whereas the holes in the valence band become trapped at the surface-bounded-OH and water molecules form •OH radicals. The degradation of dyes or other organic pollutants can be produced via two routes. The first

Additional Supporting Information may be found in the online version of this article.

one is a direct oxidation by holes on ZnO surface while the second is an indirect oxidation using hydroxyl and superoxide radicals. An undesirable route is the recombination of electrons and holes, which dissipates the energy adsorbed as heat and reduces, or even inhibits, the photocatalytic activity. Here, the charge separation (e^-–h^+) and the diffusion of the pollutant are the rate-determining steps. The role of AgNPs is to enhance ZnO photocatalytic activity since they act as electron sinks, improving the carrier-charges separation and increasing the half-life time of the primary (excited electrons and holes, e^*–h^+) and secondary (free radicals, •OH) active species. At the same time, the subsequent transfer of the trapped electrons to the adsorbed O_2 is also increased, thus producing additional free radicals and inducing a positive effect on the photocatalytic performance of ZnO.

In spite of a series of specific advantages of silver-modified ZnO particles (Ag/ZnO) (e.g., decreased charge-carriers recombination rate, photostability, low cost, and nontoxicity), its application to pilot scale systems has not been yet exploited because of difficulties associated with its recovery. The design of composites inside of which the photocatalyst is homogeneously dispersed and both water and pollutants can easily diffuse is an interesting approach for water decontamination. The composite should allow maintaining the availability of the reactive sites and, consequently, their efficiency while reducing the photocatalyst leaching. Most of the works concerned immobilization of TiO_2 into polymeric matrices applied on the degradation of dyes.[21–24] In order for a matrix to be suitable for photocatalytic water treatment under UV/visible light irradiation, in batch or continuous reactors, it must be hydrophilic, transparent, photochemically stable and mechanically resistant. For these reasons, the polyacrylates are suitable candidates for immobilizing ZnO photocatalyst. Indeed, acrylic polymers are hydrogels that allow effective water transport for contact with the target pollutants because of their hydrophilicity and high wettability, displaying a capacity to absorb large amounts of water. In addition, they are generally colourless and visually transparent, which allows the penetration of light into the matrix. Moreover, the modification of their functional groups (-COOH) could lead to selective sorption matrices.[22] For instance, the chemical interaction between polyacrylates and ZnO has been reported to be preferential.[25–27] Poly(acrylic acid) (PAA) molecules preferentially adsorb on the nonpolar facet of ZnO forming coordinative bonds between the carboxylic acid groups and Zn-atoms.[27] The photocatalytic activity of pure ZnO has been recently associated with polar facets.[28,29] This is relevant because theoretically the photoactive sites on ZnO-polyacrylates composites could be available for contaminants degradation.

Bisphenol-A (BPA) (the EDC studied in the present work), was detected in the environment for the first time in the 1930's. It came out as an estrogenic drug used for birth control, then used as a monomer in the synthesis of polycarbonate and as an additive in the synthesis of polyvinylchloride, polyesters, epoxy resins, lacquer coatings, etc. The extensive use of plastic containers made of polycarbonate, for foods and beverages, facilitates its worldwide spread. Many studies have quantified BPA levels in various aqueous media, including fresh and marine surface waters, treatment plant influents and effluents, and groundwater.[30,31] For instance, surface-water concentrations of BPA in the United States range from 0.147 to 12 mg L^{-1}.[32,33] Additionally, higher BPA concentrations are associated to wastewaters from urbanized and industrial locations. Those concentrations could become higher than the safe concentration for aquatic organisms (1.5 and 0.15 μg L^{-1}) for freshwater and marine waters, respectively).[34] Note that, biodegradation of BPA by microorganisms,[34] as well as its photochemical degradation, produce metabolites that are stable and sometimes toxic to marine species.

In this article, a novel strategy is proposed to disperse and immobilize Ag/ZnO nanoparticles in a partially cross-linked PAA matrix. However, because of their hydrophobic surface and high surface energy, these nanoparticles cannot easily disperse uniformly in the polymer matrix causing aggregation. Accordingly, Ag/ZnO nanoparticles will be firstly treated with a silane coupling agent, (3-Glycidyloxypropyl)trimethoxysilane (GLYMO) to limit the aggregation development and to introduce organic functional groups on the surface of Ag/ZnO. Secondly, after dispersion of the modified particles, Ag/ZnO-PAA composites will be synthesized by radical polymerization of acrylic acid in water, in presence of a cross-linker. The resulting composites will be characterized by several techniques including environmental scanning electron microscopy (ESEM), elemental analysis and mapping by EDS coupled to ESEM, Fourier transform infrared spectroscopy (FTIR), X-ray diffraction (XRD), and thermogravimetric analysis (TGA). Then, they will be tested and compared to pure Ag/ZnO for the photodegradation of BPA in water.

The novelty of this work, with respect to others in the field, lies mainly (i) in the surface modification of the nanoparticles to make easier their dispersion within the matrix and, (ii) in the choice of the hydrophilic and transparent cross-linked PAA matrix inside of which the particles could be anchored, allowing the UV irradiation activation of the photocatalyst. To our knowledge, this work is the first related to the photocatalytic degradation of BPA using Ag/ZnO-PAA composites.

EXPERIMENTAL

Materials

Ag/ZnO particles were previously prepared using zinc oxide nanoparticles (VP AdNano ZnO 20 DW, Degussa, Essen, Germany) and AgNPs water stabilized by an anionic surfactant (CITD-Peñoles, Torreon, Mexico).[35] HCl (38%), NaOH, acrylic acid (99%), potassium persulfate (KPS), sodium metabisulfite (98%) (SMBS), ethanol, acetonitrile (>99.8% HPLC), and BPA (2,2-bis(4-hydroxyphenyl)propane)) (>99%), were purchased from Sigma-Aldrich (St. Louis, USA). N,N′-Methylenebisacrylamide (cross-linker: MBA) (97%) and (3-Glycidyloxypropyl)trimethoxysilane (98%) (coupling agent: GLYMO) were provided by Dupont, Alfa Aesar and Dynasilan Evonik, respectively. These components were used as received without further purification.

Polymerization Set up

A triple-necked glass reactor (100 mL) was used for the synthesis of pure PAA hydrogel and Ag/ZnO-PAA composite. It was equipped with a condenser, a thermocouple and oil bath (SilOil

P20.275.50, Huber). A nitrogen flow (15 mL min^{-1}) removed oxygen during polymerization. An ultrasonic processor (power 100 W, amplitude 55%) from Hielsher Ultrasound Technology allowed dispersing the photocatalyst.

Synthesis Procedure

The immobilization of Ag/ZnO nanoparticles was carried out through (i) the surface modification of Ag/ZnO by reaction with the coupling agent, GLYMO and (ii) the synthesis of partially cross-linked PAA carried out in the presence of the modified Ag/ZnO and the cross-linking agent, MBA.

Ag/ZnO Surface Modification. Ag/ZnO nanoparticles, previously obtained by a photodeposition (PD) method and thoroughly characterized,[35] were modified using the coupling agent (GLYMO) as follows: 0.20 g of Ag/ZnO and 0.3 mL of GLYMO were dissolved in 3 mL of an ethanol-water (50/50 v/v) solution and sonicated in a beaker for 40 min at 55 °C. After washing with ethanol by several centrifugation/redispersion cycles (10 min; 3000 rpm), the recovered solids (Ag/ZnO-GLYMO) were dried at room temperature for 16 h and then at 70 °C for 16 h in a vacuum oven before use.

Syntheses of Pure PAA Hydrogel and Ag/ZnO-PAA Composites. Pure PAA hydrogel was synthesized in the triple-necked reactor using 2.5 mL of acrylic acid dissolved in 22.5 mL of deionized water. The solution was stirred and heated at 68 °C under N_2 atmosphere. Then, 0.01 g of KPS was added to initiate the polymerization. After 9 min., 0.056 g of cross-linker (MBA) and 0.005 g of second initiator (SMBS) were added. The temperature was maintained at 68 °C for 2 h and at 77 °C for 1 h. During cross-linking, the increase of viscosity was important and the product stopped quickly flowing (gel point). The gel time (around 10 min.) was reached when the hydrogel was completely formed. SMBS was used to reduce the residual monomer content in the final product. The residual reaction components were removed by immersion of the composites into an excess of water during 48 h. Finally, the resulting PAA was dried at room temperature for about 72 h, then at 65 °C for 24 h in a vacuum oven and stored.

For the synthesis of Ag/ZnO-PAA composite, Ag/ZnO-GLYMO was first vigorously dispersed in deionized water, using the ultrasonic processor, during 1 h, under vacuum to remove oxygen. The degassed suspensions and acrylic acid, previously dissolved in water, were then introduced into the triple-necked reactor and the acrylic acid polymerization was carried out under the same operating conditions as those used for the pure hydrogel synthesis. Several syntheses were carried out using 0.126 g to 0.28 g (i.e. 5% to 11% w/w based on acrylic acid) of photocatalyst therefore colouring the sample into brown hydrogel (see Supporting Information Figure S1). The obtained Ag/ZnO-PAA composites will be denominated as % composites.

Characterization of Ag/ZnO and Ag/ZnO-PAA Composite

Analytical Techniques and Sample Preparation. The samples required for analyses were dried at 80 °C, overnight, in a vacuum oven, the day before those analyses, until constant weight, and stored under vacuum.

Fourier Transform Infrared Spectrometry. A FTIR-ATR spectrophotometer (ALPHA-P Bruker) was used for the chemical analysis of pure and modified Ag/ZnO, PAA, and composites. The spectra were recorded using 4 cm^{-1} resolution over 24 scans.

Environmental Scanning Electron Microscopy. Structural and textural properties of hydrogel and composites were observed by ESEM under low vacuum (100–130 Pa), using an environmental scanning electron microscope (ESEM QUANTA 200, FEI, working with an accelerating voltage of 25 kV). The samples were (i) hydrated overnight, (ii) cut in small cubes which were placed in an aluminum pin of concave shape to maintain humidity in the microscope chamber, and (iii) immediately imaged. The analysis time did not exceed 30 min from the time that the samples were dried. Elemental analysis and mapping was carried out using Energy dispersive spectroscopy (EDS from EDAX) coupled to ESEM.

X-ray Diffraction. The X-ray analysis was made using a XRD diffractometer (BRUKER D8 from Advance) equipped with a CuKα anode (35 kV, 25 mA), in 2-theta range of 20–80°, at a scanning rate of 0.02° s^{-1}. Approximately 1 g of dry powder sample was put on the sampler forming a thin layer.

Thermogravimetric Analysis. The thermal stability of the composites was evaluated using a thermogravimetric analyzer (TGA/DCS 1, Mettler Toledo), under air atmosphere. Approximately 5 mg of dry sample was heated in an alumina pan with a scanning rate of 30 °C min^{-1} from 30 °C to 700 °C. During the heating, before achieving 200 °C, the curves remained horizontal guaranteeing a constant weight of the samples. So in the figures, these curves will begin at only 200 °C.

Photocatalytic Test

The photocatalytic degradation experiments of BPA were carried out in a photoreactor equipped with two UV-A lamps (Hg T-15L 15 W, Vilber), working at 365 nm with a power of 0.05 mW m^{-2}. Multiple spots stirrer plate allowed managing at least two runs in parallel. An aqueous solution of bisphenol-A (80 mL, 10 ppm) and the photocatalyst were placed in a glass flask magnetically stirred and UV-A irradiated. The temperature was gradually increased from 20 °C to 60 °C. The pH of the solution was monitored during the photocatalytic tests using a HAch sensION+ pH31 GLP pHmeter (initial pH 12.1 after addition of 0.8 mL NaOH of 0.5*N*). Aliquots of the solution were collected at regular UV irradiation time intervals and filtered through a 0.45 µm filter. The concentration of residual BPA was followed using ultra fast liquid chromatography (UFLC, Shimadzu), using water:acetonitrile (35/65 v/v) as the mobile phase, with a rate of 1.5 mL min^{-1} and a Kinetex 2.6u C18 100A 50 mm × 4.6 mm column. The concentration of BPA was determined using a calibration curve in the range of 1 to 10 ppm. The reproducibility of the measurements was carefully tested. Their accuracy and precision were evaluated with a BPA standard at a concentration of 5 mg L^{-1}, in terms of both percent coefficient of variation, CV (%), and percent bias value. Five replicates were assayed within three days. CV (%) and percent bias value were found equal to 1.1% and −8.91%

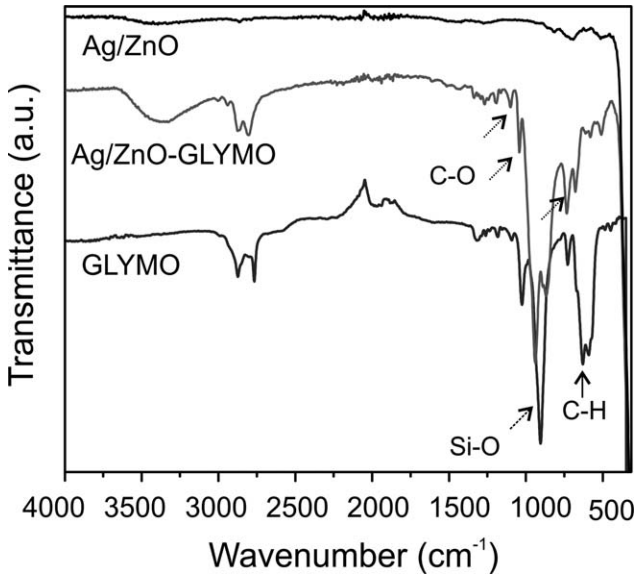

Figure 1. FTIR spectra of GLYMO, Ag/ZnO, and Ag/ZnO GLYMO.

respectively, showing that the accuracy and precision of the method was acceptable (<10% for each criterion).

RESULTS AND DISCUSSION

Synthesis and Chemical Structure of Ag/ZnO-PAA Composite

Surface modification of the nanoparticles by coupling agents has been studied recently in order to synthesize polymeric composites with a broad range of applications.[36,37] The coupling agents guarantee both the dispersion of nanoparticles as their linkage to the polymer.

Ag/ZnO Surface Modification. GLYMO is an organosilane which possesses a reactive organic epoxide and three hydrolysable methoxysilyl groups. Its use for the modification of Ag/ZnO can give rise to the formation of a silane oligolayer on the metal oxide surface and allow the development of a reaction between its hydrocarbon tail and the polymeric matrix.

The corresponding reactions were followed by FTIR spectroscopy. In the spectrum of Ag/ZnO-GLYMO (Figure 1), the peaks at 916 and 1260 cm^{-1} corresponding to epoxide functional groups indicate the presence of epoxide groups after the surface modification. However, the peak around 3400 cm^{-1} and the absence of a peak at 1660 cm^{-1} corresponding to OH groups also indicate partial hydrolysed epoxy molecules at the surface of Ag/ZnO.

The FTIR spectrum of Ag/ZnO-GLYMO shows disappearance of peaks at 823 and 780 cm^{-1}, corresponding to C-H of the methoxysilyl groups of GLYMO. This indicates hydrolysis of the methoxy groups and adsorption on the Ag/ZnO surface by weak bonds.[38] In addition, the peak at 1030 cm^{-1}, corresponding to the formation of Si-O-Si layer on Ag/ZnO surface, confirms the silanization of the photocatalyst preventing aggregation by means of steric hindrance. It was proposed that oxygen binds with the zinc surface and that the condensation results in the formation of a self-assembled monolayer (Si-O-Si).[37]

Accordingly, the mechanism of silanization of Ag/ZnO using GLYMO is summarized in Figure 2 by (i) the hydrolysis of the methoxysilyl groups, (ii) the formation of hydrogen bridges between the silane and the hydroxyl groups of the surface of ZnO, and (iii) the condensation of the adsorbed molecules, in which the oxygen binds with the Zn^{2+}-ZnO surface to form very stable structures. Part of the epoxy groups might be hydrolysed because of the modification conditions; however, the remaining epoxy groups of GLYMO are available to assist in the compatibility with the polymeric matrix.

Ag/ZnO–PAA Synthesis. FTIR spectra of pure PAA hydrogel and Ag/ZnO-PAA composite, synthesized with different photocatalyst contents, are shown in Figure 3.

The broad band around 3300 cm^{-1} is attributed to N-H functional groups of the cross-linking agent. The broad signals ranging from 3800 to 3000 cm^{-1} can also be associated to hydrogen bonds corresponding to the hydroxyl groups of poly (acrylic acid) and the humidity of the sample. The peaks at 1400, 1700, and 2940 cm^{-1} correspond to the characteristic carboxyl (C-O), carbonyl (C = O), and -CH_2 groups of PAA, respectively.

The FTIR spectra of Ag/ZnO-PAA composites show peaks similar to those of pure PAA hydrogel. In addition, a new intense peak at 1540 cm^{-1} was assigned to the ionized carboxylate groups (COO^-). The ionization of carboxylate groups in partially neutralized PAA has also been reported, where the H^+ ions of carboxylic groups in the backbone chains are irreversibly replaced by Na^+.[39] In the present study, the cationic ions are provided by ZnO-Zn^{2+} in the acidic medium during the polymerization, resulting in conditions of partial neutralization. In

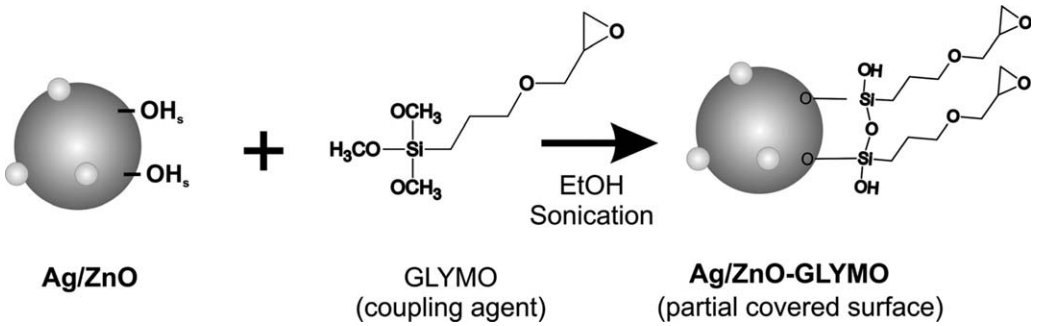

Figure 2. Mechanism proposed for the silanization of Ag/ZnO.

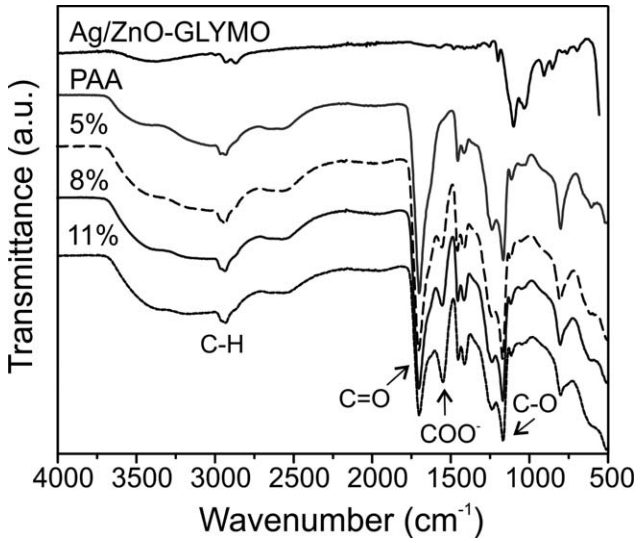

Figure 3. FTIR spectra of pure PAA hydrogel and Ag/ZnO-PAA composites synthesized with 5%, 8%, and 11% Ag/ZnO-GLYMO.

support to this claim, a new peak at 1582 cm^{-1} in the spectra of PAA/Fe_3O_4 composites, obtained by impregnation coupled to an ultrasound treatment, was reported. The appearance of this peak supports the existence of chemical interactions between the surface of the nanoparticles and PAA, leading to the formation of a cross-linked structure.[40] Bridges were suggested between carboxyl groups of one chain and several nanoparticles. On the other hand, the formation of ester-like linkages with the bare ZnO surface –(C = O)-O-(ZnO) were also proposed.[41]

In the present study, the direct interaction of PAA with the bare Ag/ZnO surface was considered less probable, because of the steric hindrance created by the attached GLYMO. However, as shown in Figure 4, the physical trapping of Ag/ZnO nanoagglomerates between entanglements remains feasible. Interaction between the free tail of GLYMO (highly reactive epoxy groups) and the carboxylic groups of PAA chains is also possible through esterification reactions, which can contribute to gel formation.[42]

Three possible arrangements can be proposed (Figure 4), where the photocatalyst is (i) attached as a pendent group to the PAA chain, (ii) linked to two PAA chains forming a cross-linked like structure and creating a bridge between the two PAA chains, and (iii) a physically trapped between PAA chain entanglements.

Structural and Textural Properties of Ag/ZnO-PAA Composite Surface Morphology Analysis. ESEM technique allows collecting electron micrographs of wet, oily, and nonconductive specimens in their natural state, without modification or preparation such as freeze-drying of samples swollen with deionized water.[43] It can show interesting details, such as the porous structure of swollen polymer networks.

In the present analysis, Figure 5 shows the irregular 3D structure of the swollen (A) and partially crashed (B) and (C) cross-linked PAA, respectively, with pores whose diameters depend on the humidity of the sample (see more details in Supporting Information Figure S2).

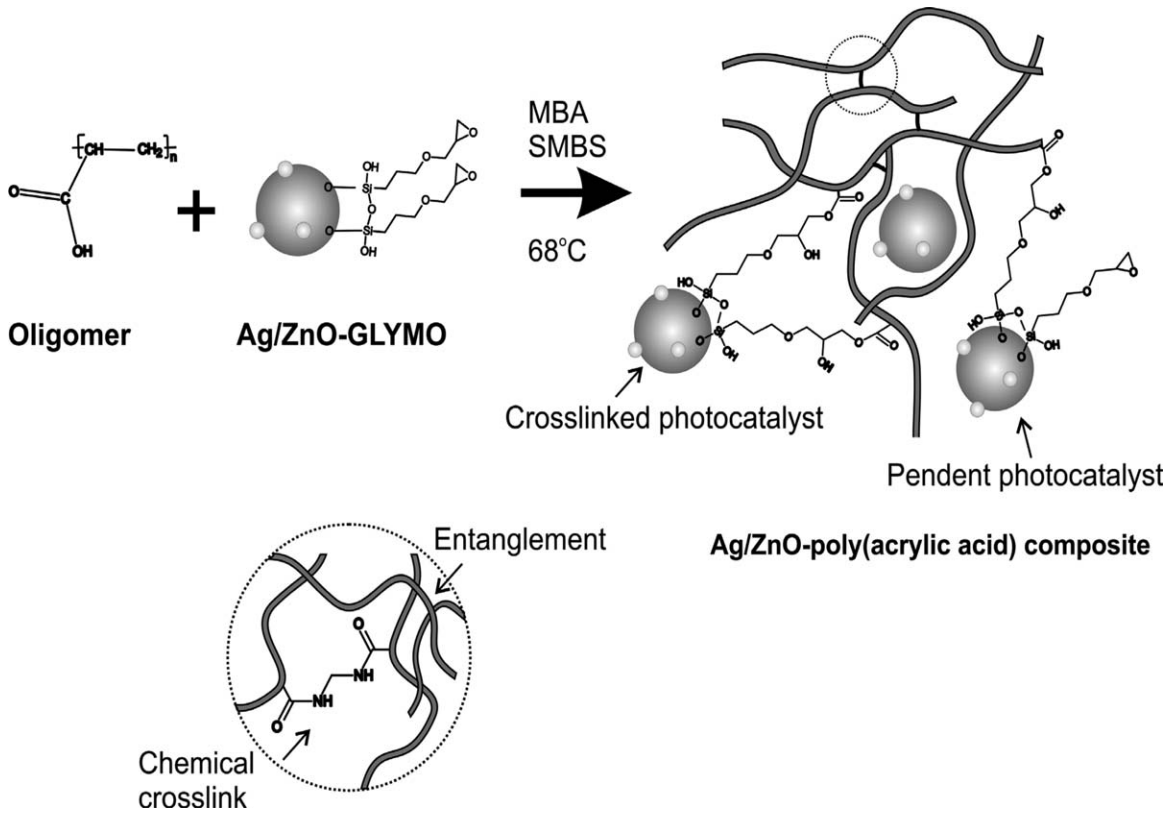

Figure 4. Scheme of the synthesis of Ag/ZnO-PAA composites.

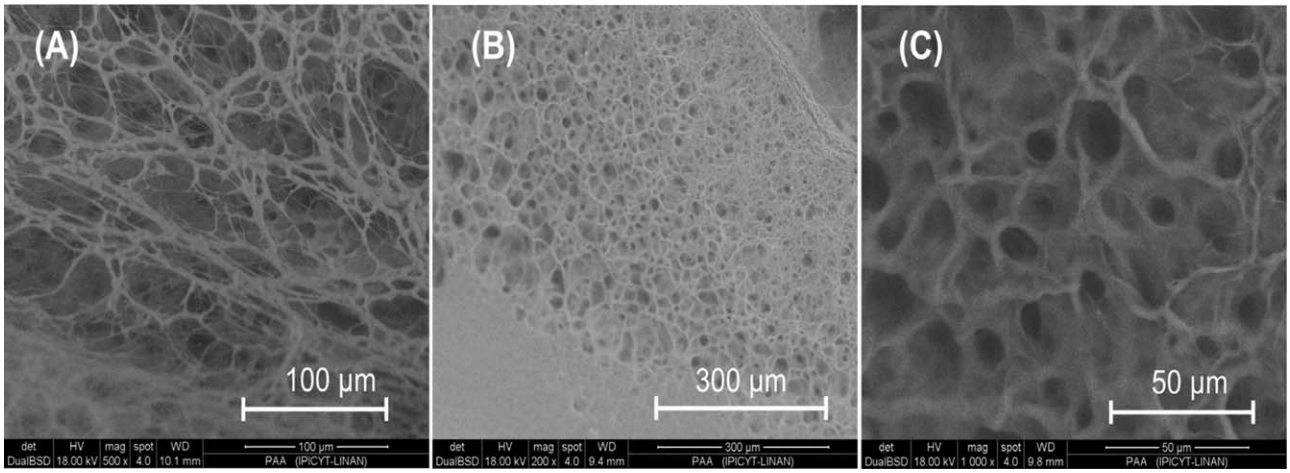

Figure 5. ESEM images of the 3D structure of (A) swollen and (B) partially crashed, and (C) cross-linked PAA.

Moreover, image (C) clearly shows that the pores of the partially crashed matrix are large enough (> 10 µm) to allow the diffusion of water and BPA molecules, whose molecular length is 1.068 nm).

The ESEM images of the Ag/ZnO-PAA composite (Figure 6) show that the nanoparticles are dispersed as islands on both 8% and 11% Ag/ZnO-PAA composites.

The chemical analysis by EDS coupled to ESEM, realized on the 11% composite, corroborates the homogenous dispersion of the photocatalyst (Supporting Information Figure S4). This suggests that the synthesis method used in this work allows the immobilization and a homogeneous distribution of the photocatalyst in the polymeric matrix. Furthermore, the porous structure of the

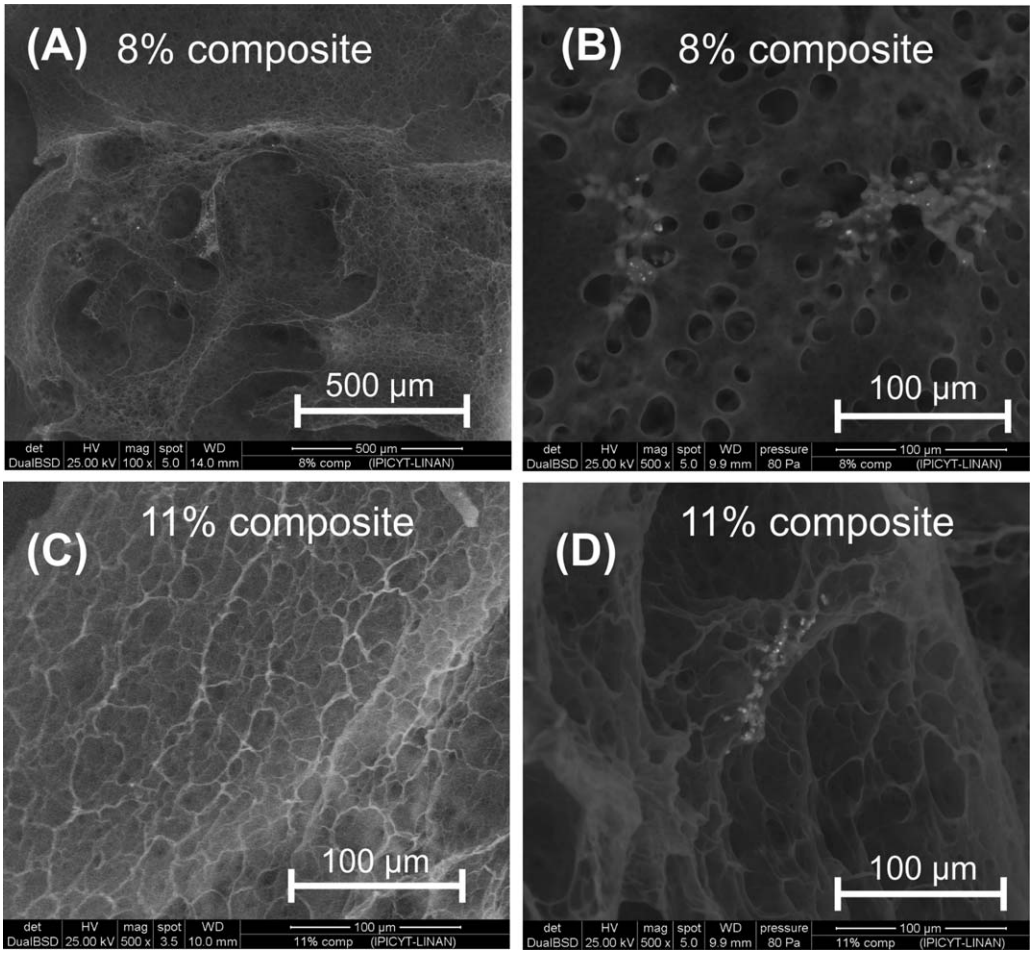

Figure 6. ESEM images of swollen Ag/ZnO-PAA composites. (A) and (B): 8% composite and (C) and (D): 11% composite.

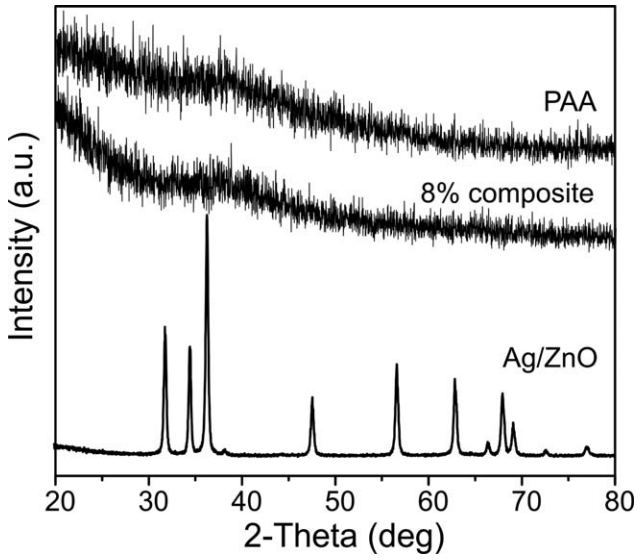

Figure 7. XRD patterns of Ag/ZnO, pure cross-linked PAA and 8% Ag/ZnO-PAA composite.

composites allows the free diffusion of BPA and interaction with the photocatalyst.

X-ray Diffraction Analysis. X-ray diffraction measurements were carried out in order to examine the effect of the photocatalyst content on the crystalline nature of the composites. XRD patterns for pure cross-linked PAA, Ag/ZnO nanoparticles and 8% Ag/ZnO-PAA composites are shown in Figure 7.

Little is known regarding the crystalline structure of PAA. XRD patterns of a PAA/ZnO nanocomposite film showed a peak at 52°, which was ascribed to the organic component (PAA).[41]

In the present work, this peak was neither observed for pure cross-linked PAA nor for the 8% composite. The absence of peaks confirmed the amorphous structure of PAA.

The diffraction peaks in XRD patterns of Ag/ZnO powder have been indexed to the hexagonally wurtzite structured ZnO which are consistent with the standard values for ZnO, given in the International Center for diffraction data, JCPDS (No. 36-1451). The significant peaks at 31.9°, 34.6°, 36.4°, 47.7°, 56.7°, 63°, 66.5°, 68.1°, 69.2°, 72.7°, and 77.1° are in agreement with the reported peaks for ZnO corresponding to the (100), (002), (101), (102), (110), (103), (200), (112), (201), (004), and (202) diffraction patterns, respectively. In addition, the peak at 38.3°, which is in agreement with the reported peak for metallic Ag, corresponding to the crystalline plane (111) (card JCPDS 04-0783), confirms the presence Ag in Ag/ZnO.

Although the XRD pattern of the 8% composite showed a broad peak at low angles, the diffraction peaks of ZnO were not clearly observed on it, probably because of its low Ag/ZnO content.

Thermogravimetric Analysis. Figure 8 shows TGA thermograms of Ag/ZnO-GLYMO, PAA, 5%, and 8% composites obtained under air atmosphere treatment (See Supporting Information Figure S5 for N_2 treatments). Analysis of those traces clearly shows that the thermal stability of the PAA matrix is improved by the addition of Ag/ZnO nanoparticles. It was demonstrated that among several composites of PAA-metal oxides such as ZnO, CaO and CuO, the PAA-ZnO composite was the most thermally stable.[26] Similar results were obtained for the P(AA-SA)/ZnO composite containing 11 wt % of ZnO nanoparticles.[44]

The weight loss of Ag/ZnO-GLYMO between 250 °C and 550 °C (6.14 wt %) is attributed to the thermal decomposition of the Si-O-Si layer. This corroborates the silanization of Ag/ZnO surface proposed in Figure 2. Similar results were reported on rutile TiO_2 particles grafted with GLYMO.[45]

Structure Photostability. It has been reported that composites based on polyacrylates can be degraded by (i) photocleavage and (ii) oxidation initiated by photocatalytic reactions.[21]

To check the influence of the irradiation on the composite photostability, a sample of the 8% Ag/ZnO-PAA composite, containing approximately 10 ppm of BPA, was irradiated during 8 h under UV-A light ($\lambda = 365$ nm).

FTIR and TGA analyses were carried out on the sample before and after irradiation (Figure 9). The two FTIR spectra obtained [Figure 9(A)] are identical, which demonstrates that the chemical structure of the composite remains unaffected after this irradiation. This is confirmed by the presence, after irradiation, of the peak around 500 cm^{-1} attributed to Zn-O.

On the other hand, TGA thermograms [Figure 9(B)] showed a higher residual mass after irradiation (30.59 wt % against 20.19 wt % before irradiation). The difference can be because of the accumulation of by-products resulting from BPA photodegradation and polymerization during the photocatalytic process, as suggested by other authors.[46]

Photocatalytic Efficiency of Ag/ZnO-PAA Composites

During an initial set of experiments under conditions of darkness, the concentration of BPA changed slightly within 3 h. This indicates that a small fraction of BPA is sorbed by the

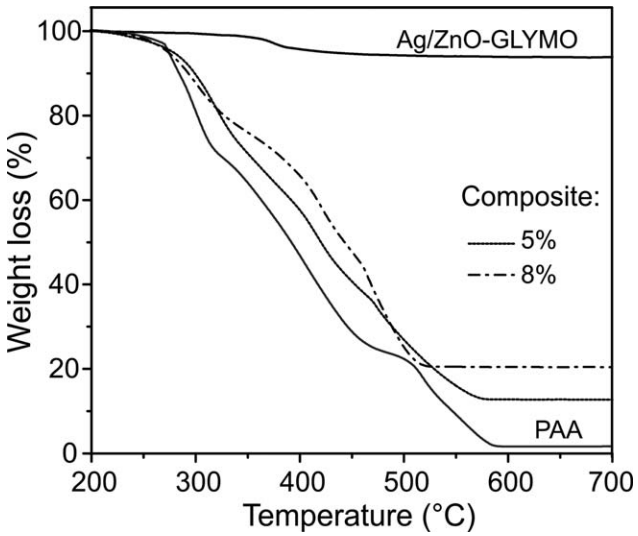

Figure 8. TGA curves of Ag/ZnO-GLYMO, pure cross-linked PAA, 5%, and 8% Ag/ZnO-PAA composites.

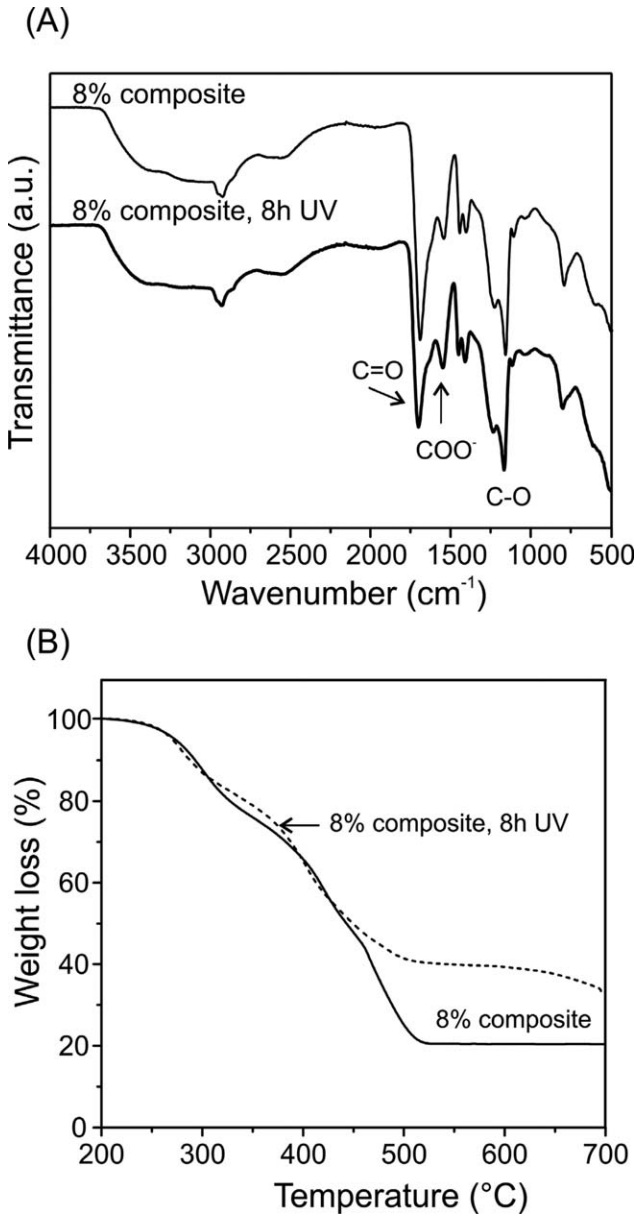

Figure 9. FTIR (A) and TGA (B) spectra of 8% Ag/ZnO-PAA composite before and after 8 h of UV irradiation.

composite. Figure 10(A) and Table I show the corresponding photocatalytic performance of the composites.

More precisely, Figure 10(A) shows the time evolution of $-\ln(C/C_0)$ which follows a pseudo-first order kinetic, $(-\ln(C/C_0)=K_{app}t)$, where C_0 and C are the BPA concentrations at irradiation time t zero and different irradiation times up to 8 h, respectively, and K_{app} is the apparent rate constant of BPA degradation.

Using Ag/ZnO-PAA the apparent rate constant K_{app} (0.1129×10^{-2} min^{-1}) is greater than that of pure PAA (0.0451×10^{-2} min^{-1}). Although this apparent rate constant is inferior to the one obtained using Ag/ZnO-GLYMO under the same operating conditions (0.2942×10^{-2} min^{-1}), it becomes evident that the immobilization of the photocatalyst can achieve comparable photodegradation efficiencies while providing a series of additional advantages at the same time (e.g., reduced photocatalyst loss and possibility to implement to continuous systems).

Furthermore, the degradation of BPA increases as the Ag/ZnO-GLYMO content in the composite increases: 8% > 5% ≫ pure PAA. The overall achieved photodegradation percentages of BPA in the framework of this work are comparable to those reported in the literature under similar reaction conditions using composites. For instance, 80% of degradation of BPA (11.4 ppm) in 24 h using TiO_2/zeolite,[47] and 75% of degradation of BPA (15 ppm) using TiO_2/carbon in 5 h.[48] In the present study, 47% of BPA (10 ppm) was decomposed in 8 h using the 8% Ag/ZnO-PAA composite.

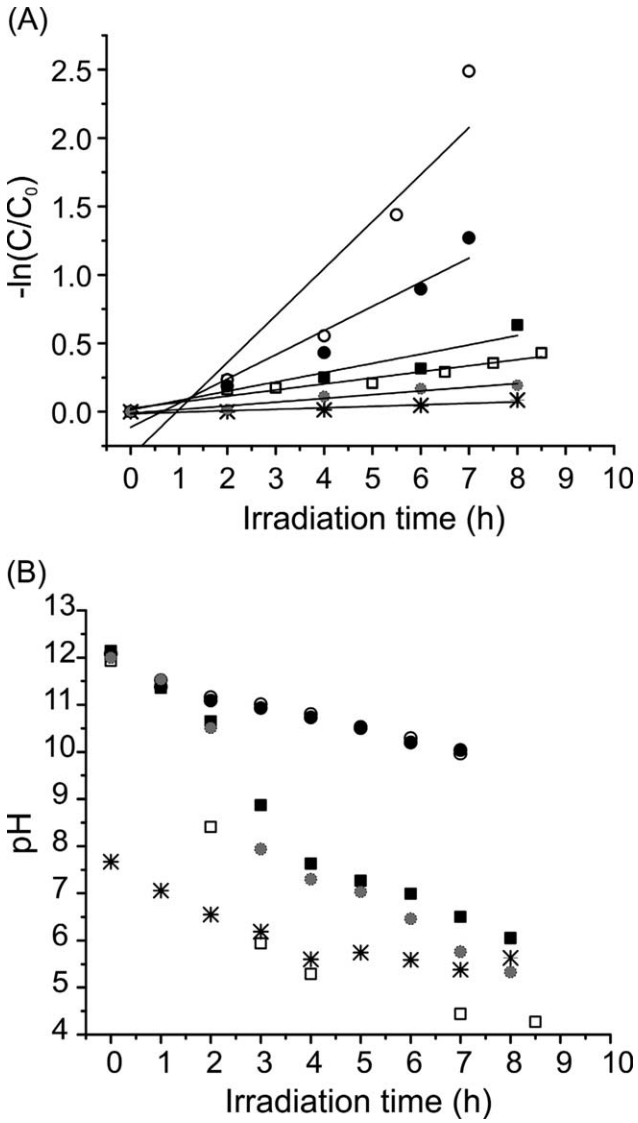

Figure 10. Pseudo-first order kinetics of (A) photocatalytic degradation of BPA and (B) time evolution of the pH of the solution, using Ag/ZnO-GLYMO and Ag/ZnO-PAA composites (BPA = 10 ppm, $\lambda = 365$ nm, initial pH = 12.1). (○) Ag/ZnO-GLYMO 0.1875 g/L, (●) Ag/ZnO-GLYMO 0.27 g/L, (□) 5% composite, (■) 8% composite, (●) pure cross-linked PAA and (∗) photolysis (UV only).

Table I. Degradation of Bisphenol-A: Pseudo-First Order Apparent Rate Constants

Sample	Bisphenol-A degradation (%)	$K_{app} \times 10^{-2}$ (min^{-1})	R^2
Ag/ZnO-GLYMO 0.1875 g/L	91.69	0.5179	0.8687
Ag/ZnO-GLYMO 0.27 g/L	71.94	0.2942	0.9394
5% composite	34.95	0.0739	0.9491
8% composite	46.93	0.1129	0.8819
PAA	17.61	0.0451	0.9491
Photolysis (UV only)	8.20	0.0182	0.8754

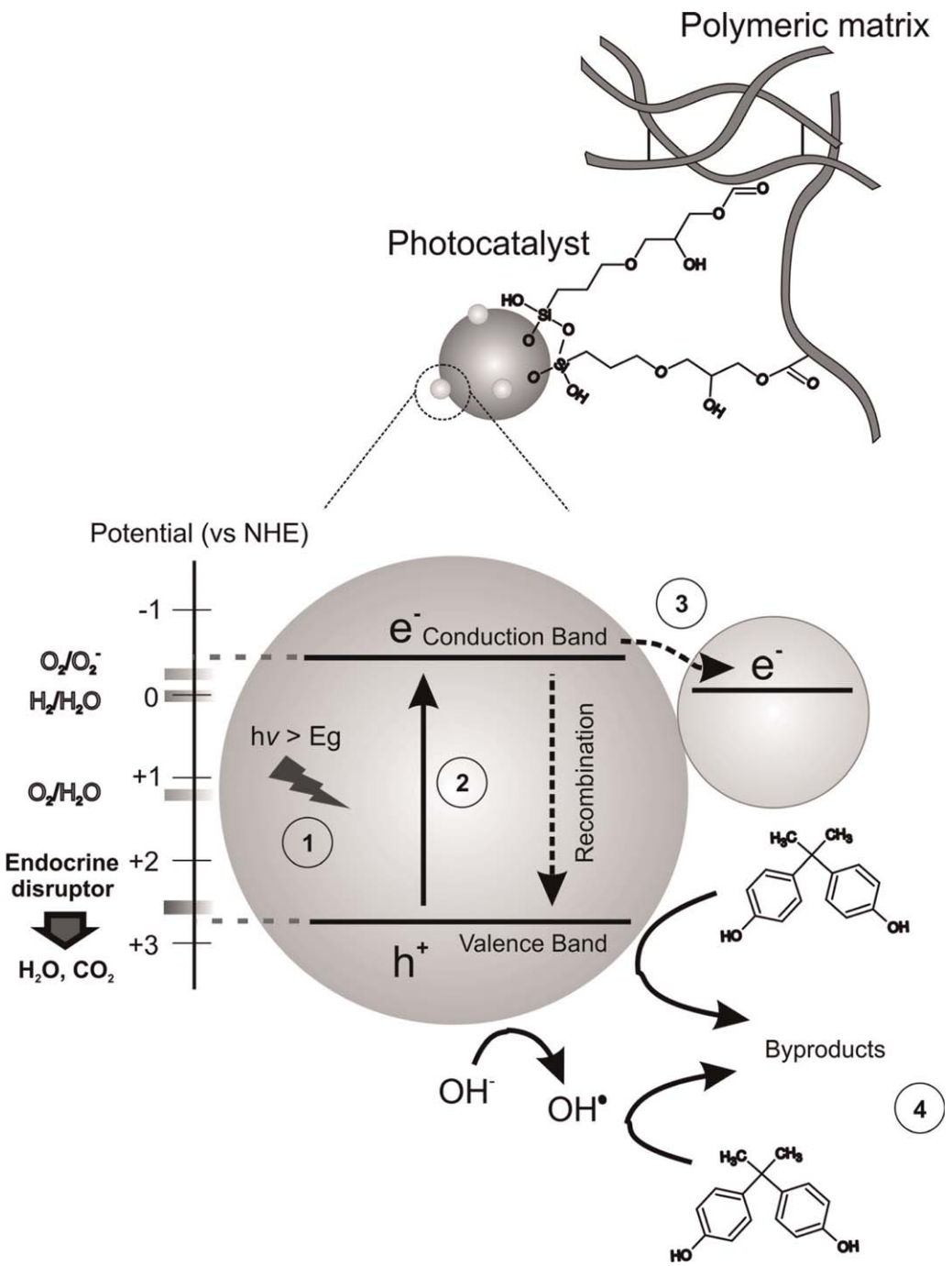

Figure 11. Scheme of the mechanism proposed for the photocatalytic degradation of BPA using Ag/ZnO-PAA composites considering the theoretical approach described in the introduction.

Figure 10(B) shows that the pH of the solution decreases as the irradiation time increases. This could be attributed to the formation of acidic intermediate byproducts. Indeed, some byproducts were observed, but not identified, in the HPLC chromatograms, at lower retention times than BPA (see Supporting Information Figure S6). The pH of the solution depends on the amount of the surface charges of PAA and BPA. BPA pK_a is 10.1, meaning that nonionized molecules (HO-$C_{15}H_{14}$-OH) prevail in neutral and acidic conditions. On the other hand, the pk_a of carboxylic acid groups is around 4.0. Hence, when the value of pH is higher than 4.0, the carboxyl groups of PAA are ionized forming -COO^- groups. This enhances the affinity of PAA with water. In the present work, NaOH was used at the beginning of the experiments, in order to increase PAA/water affinity and swelling. Under these conditions, the repulsion forces between PAA and BPA are very weak. Therefore, in the swollen composite, the 3D structure of PAA allows the penetration and the diffusion of BPA molecules. Once into the matrix, the BPA molecules can be destroyed, according to the mechanism already described in the literature.[49–51]

Accordingly, considering the theoretical approach described in the introduction for the photodegradation of dyes and other organic pollutants, Figure 11 proposes the mechanism for the photocatalytic degradation of BPA.

Furthermore, in an attempt to deepen the photocatalytic activity of the composites, both 5% and 8% Ag/ZnO-PAA composites were re-used in a second cycle of 8 h UV irradiation, without washing. The results show that the photocatalytic activity of the samples was kept relatively constant, leading to an overall photodegradation of BPA equal to 37% and 41% for the 5% composite and to 47% and 64% for the 8% composite, after the 1st and 2nd cycles, respectively.

Since the chemical structure of the composite remained also unaffected after 8 h of UV light exposure, those last results suggest that the photocatalyst immobilization in the PAA matrix allows preventing Ag/ZnO photocorrosion and therefore maintaining its photocatalytic activity. Also, the increased activity for the second cycle, can be attributed to a more exposed photocatalyst that is located into the polymeric matrix. Similar results showed that polyaniline suppressed the ZnO photocorrosion during methylene blue degradation under UV light.[52]

CONCLUSIONS

This work aimed to understand and improve the photocatalytic efficiency of ZnO over the photodegradation, in batch and continuous systems, of water contaminants, particularly endocrine disrupting compounds such as BPA. It is part of a wider study made of three complementary steps related to:

- the synthesis of Ag/ZnO nanoparticles,[35]
- their immobilization inside of a cross-linked PAA matrix, and
- the evaluation and the optimization of the photocatalytic activity of the obtained Ag/ZnO-PAA composite.[53]

As described in a previous paper,[35] the synthesis of Ag/ZnO nanoparticles, realized by loading stabilized silver nanoparticles (AgNPs) on ZnO surface, clearly demonstrated the positive effect of AgNPs on the photocatalytic performance of ZnO.

The present work concerns the dispersion and the immobilization of Ag/ZnO nanoparticles in a PAA matrix. However, because of their hydrophobic surface and high surface energy, these nanoparticles, were firstly treated with a silane coupling agent, (3-Glycidyloxypropyl)trimethoxysilane (GLYMO) to limit their aggregation and to introduce organic functional groups on their surface. FTIR analysis of the modified photocatalyst allowed proposing the mechanism of the silanization including:

- the hydrolysis of the silane methoxysilyl groups,
- the formation of hydrogen bonds between the silane and the hydroxyl groups of the surface of ZnO, and
- the condensation of the adsorbed molecules to form very stable structures.

The immobilization of the silanized Ag/ZnO nanoparticles was then carried out by vigorously dispersing Ag/ZnO nanoparticles (5–11 wt % content) in a water solution of acrylic acid and polymerizing the acrylic acid in the presence of two initiators (potassium persulfate and sodium metabisulfite) and a cross-linker (N, N-methylenebisacrylamide).

The chemical structure of the obtained Ag/ZnO-PAA composites was followed by FTIR spectroscopy. The results allowed proposing an esterification reaction between the opened ring of the epoxy group of Ag/ZnO-GLYMO and the carboxylic group of PAA, suggesting three possible arrangements of the photocatalyst inside of the polymer matrix: (i) attached as a pendent group to the PAA chain, (ii) linked to two PAA chains forming a cross-linked like structure and creating a bridge between the two PAA chains, and (iii) a physically trapped between PAA chain entanglements.

The structural and textural properties of Ag/ZnO-PAA composites were then analyzed in terms of morphology, crystalline structure, thermal degradation, and photostability. ESEM images clearly showed the porous structure of the composites while analysis by EDS coupled to ESEM confirmed the rather good dispersion of the photocatalyst in the matrix. Moreover, the composites presented the advantages of transparency, hydrophilicity, and photostability to afford photodegradation of contaminants dissolved in aqueous solutions.

The resulting composites were then successfully tested in a batch reactor configuration for the degradation of BPA under UV light ($\lambda = 365$ nm).

The results showed that the corresponding photocatalysis follows a pseudo-first order kinetic and demonstrate that the composites can achieve photodegradation efficiencies comparable to the ones obtained by pure Ag/ZnO.

They provide additional advantages such as reduction of photocatalyst loss and reuse of the composite for the degradation of BPA.

The possibility to implement this new type of photocatalyst in continuous systems for the degradation endocrine-disrupting compounds dissolved in water is another advantage of the proposed photocatalyst.

ACKNOWLEDGMENTS

The authors thank the CONACYT-Mexico and the French Ministry of Education and Research for the scholarship PCP/RUI-004-12 granted to Alma B. Jasso-Salcedo. They acknowledge the technicians of LINAN laboratories in IPICYT and ENSIC laboratories from Lorraine University for technical support on characterization.

REFERENCES

1. Westerhoff, P.; Yoon, Y.; Snyder, S.; Wert, E. *Environ. Sci. Technol.* **2005**, *39*, 6649.
2. Ternes, T. A.; Meisenheimer, M.; McDowell, D.; Sacher, F.; Brauch, H. J.; Haist-Gulde, B.; Preuss, G.; Wilme, U.; Zulei-Seibert, N. *Environ. Sci. Technol.* **2002**, *36*, 3855.
3. Boyd, G. R.; Reemtsma, H.; Grimm, D. A.; Mitra, S. *Sci. Total Environ.* **2003**, *311*, 135.
4. Stackelberg, P. E.; Gibs, J.; Furlong, E. T.; Meyer, M. T.; Zaugg, S. D.; Lippincott, R. L. *Sci. Total Environ.* **2007**, *377*, 255.
5. Huerta-Fontela, M.; Galceran, M. T.; Ventura, F. *Water Res.* **2011**, *45*, 1432.
6. Keane, D. A.; McGuigan, K. G.; Ibanez, P. F.; Polo-Lopez, M. I.; Byrne, J. A.; Dunlop, P. S. M.; O'Shea, K.; Dionysiou, D. D.; Pillai, S. C. *Catal. Sci. Technol.* **2014**, *4*, 1211.
7. Linsebigler, A.; Lu, G.; Yates, J. *Chem. Rev.* **1995**, *95*, 735.
8. Asahi, R.; Morikawa, T.; Ohwaki, T.; Aoki, K.; Taga, Y. *Science* **2001**, *293*, 269.
9. Takai, A.; Kamat, P. V. *ACS Nano* **2011**, *5*, 7369.
10. Kale, M. J.; Avanesian, T.; Christopher, P. *ACS Catal.* **2013**, *4*, 116.
11. Costi, R.; Saunders, A. E.; Elmalem, E.; Salant, A.; Banin, U. *Nano Lett.* **2008**, *8*, 637.
12. Wang, P.; Huang, B.; Zhang, X.; Qin, X.; Jin, H.; Dai, Y.; Wang, Z.; Wei, J.; Zhan, J.; Wang, S. *Chem. Eur. J.* **2009**, *15*, 1821.
13. Zhang, H.; Fan, X.; Quan, X.; Chen, S.; Yu, H. *Environ. Sci. Technol.* **2011**, *45*, 5731.
14. Liu, Y.; Fang, L.; Lu, H.; Liu, L.; Wang, H.; Hu, C. *Catal. Commun.* **2012**, *17*, 200.
15. Hu, C.; Lan, Y.; Qu, J.; Hu, X.; Wang, A. *J. Phys. Chem. B.* **2006**, *110*, 4066.
16. Wang, P.; Tang, Y.; Dong, Z.; Chen, Z.; Lim, T. T. *J. Mater. Chem. A* **2013**, *1*, 4718.
17. Xie, W.; Li, Y.; Sun, W.; Huang, J.; Xie, H.; Zhao, X. *J. Photochem. Photobiol. A* **2010**, *216*, 149.
18. Wang, J.; Fan, X. M.; Tian, K.; Zhou, Z. W.; Wang, Y. *Appl. Surf. Sci.* **2011**, *257*, 7763.
19. Peng, F.; Zhu, H.; Wang, H.; Yu, H. *Korean J. Chem. Eng.* **2007**, *24*, 1022.
20. Tan, S. T.; Ali Umar, A.; Balouch, A.; Nafisah, S.; Yahaya, M.; Yap, C. C.; Mat Salleh, M.; Kityk, I. V.; Oyama, M. *ACS Comb. Sci.* **2014**, *16*, 314.
21. Kangwansupamonkon, W.; Jitbunpot, W.; Kiatkamjornwong, S. *Polym. Degrad. Stabil.* **2010**, *95*, 1894.
22. Wang, S. Q.; Liu, Q. L.; Zhu, A. M. *Eur. Polym. J.* **2011**, *47*, 1168.
23. Leng, C.; Wei, J.; Liu, Z.; Xiong, R.; Pan, C.; Shi, J. *J. Nanopart. Res.* **2013**, *15*, 1.
24. Li, Y.; Yu, Y.; Wu, L.; Zhi, J. *Appl. Surf. Sci.* **2013**, *273*, 135.
25. Padilla, A.; Vazquez, A.; Vazquez-Polo, G.; Acosta, D.; Castaño, V. *J. Mater. Sci. Mater. Med.* **1990**, *1*, 154.
26. Wu, H. S.; Jone, H. C.; Hwang, J. *J. Appl. Polym. Sci.* **1997**, *63*, 89.
27. Kunze, C.; Valtiner, M.; Michels, R.; Huber, K.; Grundmeier, G. *Phys. Chem. Chem. Phys.* **2011**, *13*, 12959.
28. Zhang, L.; Yin, L.; Wang, C.; Lun, N.; Qi, Y. *ACS Appl. Mater. Interfaces* **2010**, *2*, 1769.
29. Huang, M.; Yan, Y.; Feng, W.; Weng, S.; Zheng, Z.; Fu, X.; Liu, P. *Cryst. Growth Des.* **2014**, *14*, 2179.
30. Flint, S.; Markle, T.; Thompson, S.; Wallace, E. *J. Environ. Manage.* **2012**, *104*, 19.
31. Klečka, G. M.; Staples, C. A.; Clark, K. E.; van der Hoeven, N.; Thomas, D. E.; Hentges, S. G. *Environ. Sci. Technol.* **2009**, *43*, 6145.
32. Kolpin, D. W.; Furlong, E. T.; Meyer, M. T.; Thurman, E. M.; Zaugg, S. D.; Barber, L. B.; Buxton, H. T. *Environ. Sci. Technol.* **2002**, *36*, 1202.
33. Zhang, S.; Zhang, Q.; Darisaw, S.; Ehie, O.; Wang, G. *Chemosphere* **2007**, *66*, 1057.
34. Kang, J. H.; Katayama, Y.; Kondo, F. *Toxicology* **2006**, *217*, 81.
35. Jasso-Salcedo, A. B.; Palestino, G.; Escobar-Barrios, V. A. *J. Catal.* **2014**, *318*, 170.
36. Abdolmaleki, A.; Mallakpour, S.; Borandeh, S. *Appl. Surf. Sci.* **2011**, *257*, 6725.
37. Petoral, J.,R. M.; Yazdi, G. R.; Spetz, A. L.; Yakimova, R.; Uvdal, K. *Appl. Phys. Lett.* **2007**, *90*, 223904.
38. Mallakpour, S.; Madani, M. *Bull. Mater. Sci.* **2012**, *35*, 333.
39. Bejarano-Jiménez, A.; Escobar-Barrios, V. A.; Kleijn, J. M.; Ortíz-Ledón, C. A.; Cházaro-Ruiz, L. F. *J. Appl. Polym. Sci.* **2014**, *131*, 40846.
40. Wei, S.; Zhang, Y.; Xu, J. *Front. Chem. Eng. China.* **2007**, *1*, 233.
41. Zou, S.; Bai, H.; Yang, P.; Yang, W. *Macromol. Chem. Phys.* **2009**, *210*, 1519.
42. Sun, S.; Sun, P.; Liu, D. *Eur. Polym. J.* **2005**, *41*, 913.
43. Patel, V. R.; Amiji, M. M. *Pharm. Res.* **1996**, *13*, 588.
44. Luo, Y. D.; Dai, C. A.; Chiu, W. Y. *J. Polym. Sci. Part A Polym. Chem* **2008**, *46*, 8081.
45. Godnjavec, J.; Znoj, B.; Vince, J.; Steinbucher, M.; Venturini, P. *Mater. Technol.* **2012**, *46*, 19.
46. Lu, B.; Liu, M.; Shi, H.; Huang, X.; Zhao, G. *Electroanalysis* **2013**, *25*, 771.

47. Fukahori, S.; Ichiura, H.; Kitaoka, T.; Tanaka, H. *Environ. Sci. Technol.* **2003**, *37*, 1048.

48. Kim, J.; Kwak, B. S.; Kang, M. *Bull. Korean Chem. Soc.* **2010**, *31*, 344.

49. Clament Sagaya Selvam, N.; Judith Vijaya, J.; John Kennedy, L. *J. Colloid Interface Sci.* **2013**, *407*, 215.

50. Guo, C.; Ge, M.; Liu, L.; Gao, G.; Feng, Y.; Wang, Y. *Environ. Sci. Technol.* **2009**, *44*, 419.

51. Nomiyama, K.; Tanizaki, T.; Koga, T.; Arizono, K.; Shinohara, R. *Arch. Environ. Contam. Toxicol.* **2007**, *52*, 8.

52. Zhang, H.; Zong, R.; Zhu, Y. *J. Phys. Chem. C.* **2009**, *113*, 4605.

53. Jasso-Salcedo, A. B.; Meimaroglou, D.; Camargo, M.; Hoppe, S.; Pla, F.; Escobar-Barrios, V. A. *Chem. Eng. Trans.* **2015**, *43*, 937.